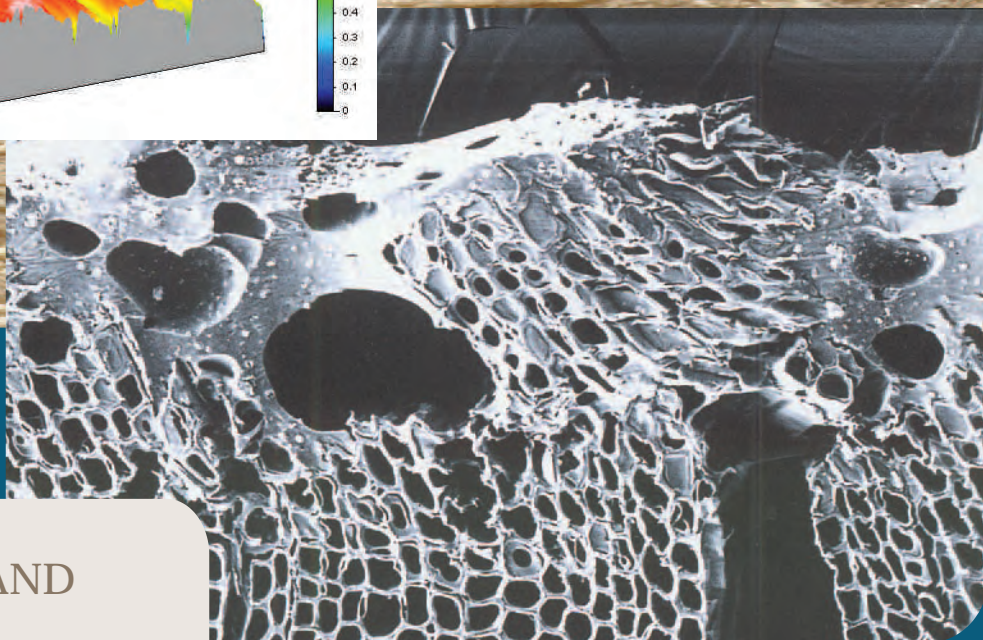
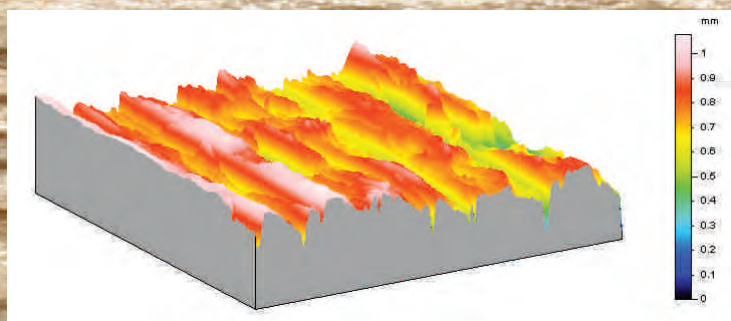


ensis

WOOD PROCESSING

ISSUE NO.38
JUNE 2006 NEWSLETTER



CRUSTACEANS AND
FUNGI

PINE BARK ADHESIVES

BAFFLED?

MORE ON MICROSCOPY
OF COATING ISSUES



REPLACING CHEMICAL WOOD ADHESIVES

Extracts from the humble pine tree could eventually replace chemical wood adhesives thanks to joint work under way by Ensis and Scion scientists. The collaboration between the two groups has allowed the technology to be fast-tracked towards commercialisation.

A team from Scion's biomaterials unit has spent the past 5 years working on extracting chemicals from pine bark and finding ways these natural chemicals could replace synthetic and petroleum-based compounds used in building products, packaging, plastics, and cosmetics.

Dr Alan Fernyhough, leader of Scion's Biomaterials Engineering unit, says it is early days for the plastics and cosmetics research, but along with Ensis Wood Processing, the team is now in the process of identifying partners to commercialise the work on wood adhesives for the building industry.



Team leader, Dr Alan Fernyhough, and General Manager, Dr Jamie Hague

The product is a high-performance adhesive that uses tannin in phenolic-resorcinol formaldehyde adhesive systems (tannin-PRF). Tannin, a natural chemical obtained from pine trees, is used to replace part of the oil-based ingredients comprising such adhesives, which are used in structural beams, in solid wood joints, and for other commercial building uses.

“We ran our first trial a couple of years ago and proved the pine derivative is a viable alternative to

synthetic chemicals. We are now working with an international company to assess the commercial opportunity for the wood adhesive technology.”

Dr Jamie Hague, General Manager of Ensis Wood Processing, says the work is of international significance.

“It is highly likely the technology being created will be adopted overseas. It would have been a lot more difficult to get to this stage without working together,” he says.

Jamie says although a great deal of international work has been done over the past 20 years, he believes the Ensis research has now reached commercialisation due to a number of new factors.

“This research is very relevant in today's society. There is a growing interest in bio-based materials and this research has particular appeal as it uses a waste material.

“I see this as just a first step towards revolutionising the wood processing industry. With respect to adhesives, the long-term goal is to develop systems that are based entirely on renewable materials, with a particular focus on eliminating formaldehyde as a component.”

Jamie says there are many advantages in using the pine tree extracts over current chemicals. Firstly, pine trees are a sustainable resource that grows well in New Zealand. Added to that, the formaldehyde emissions from the new adhesive are lower than from standard adhesives.

“We expect new adhesive and related coating formulations to emerge from a pipeline of enhanced product developments in the future. The tannin-based alternative also helps remove some of the environmental cost of using petrochemicals.

“The big advantages with the adhesive we've created for the wood processing industry are that the product is better for the environment and no new equipment is needed by factories to make it,” he says.

Contact: jamie.hague@ensisjv.com
Phone: +61 3 9546 2128

COMPARING THE WOOD PROPERTIES OF CYPRESS SPECIES

Charlie Low (*Ensis Wood Processing*)

Cypress species have been grown on New Zealand farms since around 1860, intended as a durable alternative for native timbers. In recent years the development of portable sawmills has seen increased production of cypress timber and, because of its attractive appearance, its use for higher value applications, such as kitchen joinery and boat joinery, rather than just farm gates and shed weatherboards.

Utilisation of a variety of cypress species has been investigated at Forest Research since the 1960s. More recently there have been suggestions that cypresses, grown on relatively short rotations of 20 to 25 years, could yield well-formed logs containing high proportions of naturally durable heartwood with favourable properties and appearance. Ensis set out to test this by determining the appearance and structural quality of lumber from pruned 21-year-old trees of three cypress species/hybrids — *Cupressus macrocarpa*, *C. lusitanica*, and *Chamaecyparis nootkatensis* × *C. macrocarpa* (“Leyland”). Harvesting at 21 years is considered to be around half the “normal” rotation age.

Cupressus macrocarpa has been widely planted on New Zealand farms since 1860. It has essentially replaced totara as a durable timber for farm use, and kauri as a stable timber for boat building. Due to its attractive appearance *C. macrocarpa* has been widely used in doors, joinery, and kitchens.

Cupressus lusitanica is not as well known in New Zealand as *C. macrocarpa*, but is now being planted more widely, as it is less susceptible to cypress canker fungi (*Seiridium cardinale* and *S. unicornne*). It has a reputation for greater stability on drying than *C. macrocarpa* and, while not as strong, in other respects is considered very similar.

Leyland cypress is an inter-generic hybrid between yellow cedar, *Chamaecyparis nootkatensis*, and *C. macrocarpa*, and several clones have been deployed widely by vegetative propagation. It is a healthy and well-formed cypress and has been planted in shelterbelts, but infrequently in plantations. The properties of New Zealand-grown Leyland cypress timber have been reported in *Bulletin No. 119* (1986), available through Ensis.

Early utilisation studies of *Cupressus macrocarpa* and *C. lusitanica* had shown that kiln-dried *C. macrocarpa* timber from shelterbelts suffered

extensive internal checking. Air-drying on its own, or in combination with kiln-drying, also resulted in surface- and end-checking. In contrast, *C. lusitanica* was successfully dried without internal checking or collapse using a low-temperature kiln schedule. However, checks developed within and around intergrown knots in this species, and both kiln- and air-dried boards showed end-checking. In some of the later studies, timber distortion was also encountered.

For this latest study the 21-year-old trees all came from the Rotorua area. All species were planted at 1111 stems/ha, and later pruned in stages to height 5–8 m and thinned to 550 stems/ha. Each species had some advantages and disadvantages in growth, form, and sawn timber characteristics. *Cupressus macrocarpa* had grown to the same diameter at breast height (dbh) as *C. lusitanica*, and both had grown much faster than Leyland. *Cupressus macrocarpa*, however, was the tallest but suffered badly from canker. Leyland had straighter stems than the others, and a higher frequency of branching.

Sawn-timber recovery was 50–60% for all log height classes of each species, except for the butt logs of *C. macrocarpa*, ca. 40%, owing to fluting and high taper. The sawn timber was graded using NZS 3631 appearance grading rules. From the Table it can be seen that Leyland produced the highest percentage of Dressing & Merchantable grade combined, followed by *Cupressus lusitanica* and then *C. macrocarpa*.

Percentage grade recovery, by species

Species	Dressing	Merchantable	Box
<i>C. lusitanica</i>	48	24	28
<i>C. macrocarpa</i>	33	21	46
Leyland	37	44	19

Causes of appearance degrade varied among species. The worst defect for *C. lusitanica* was knot checking. For *C. macrocarpa*, surface checking was the biggest problem, and in Leyland pruned branch stub holes caused by lack of intergrowth around the dead branch wood. Time of pruning may alleviate this problem. There was a lot of tree-to-tree variation in checking in each species. Knot checks were a serious defect in all species, which resulted in chip out of knots during machining processes.

Structurally, tests of bending stiffness for *C. lusitanica* timber showed it was less stiff than the Leyland hybrids and *C. macrocarpa*, and all were less stiff than radiata pine. Stiffness increased substantially from the inner boards to the outer in all species and increased age will undoubtedly result in an improvement in average stiffness relative to younger material. Bending strength was similar to that of

radiata pine for *C. macrocarpa* and Leyland, but *C. lusitanica* was not as strong. In addition to lower stiffness and strength, a tendency to warp (twist and crook) was also a disadvantage for *C. lusitanica*

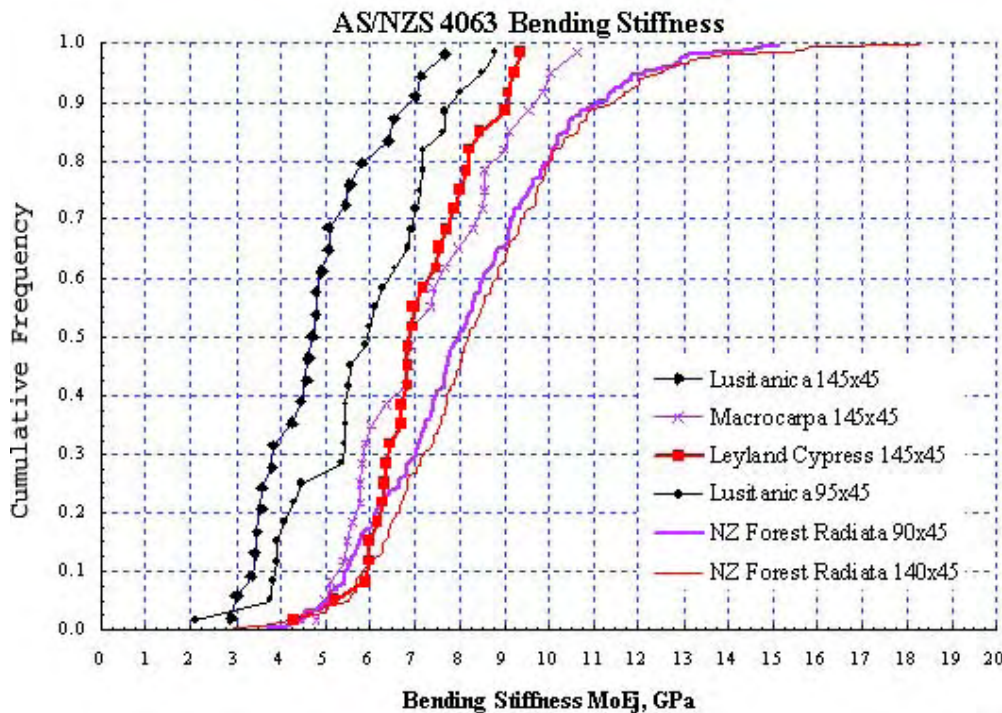
The good performance of the appearance and structural products of the four *Chamaecyparis nootkatensis* × *C. macrocarpa* hybrid clones

(Leyland) may be a pointer towards the development of faster-grown hybrids involving southern Oregon provenances of *Ch. nootkatensis*. The “ovensii” hybrid clone of *Ch. nootkatensis* × *C. lusitanica* is reputed to grow fast and be resistant to canker.

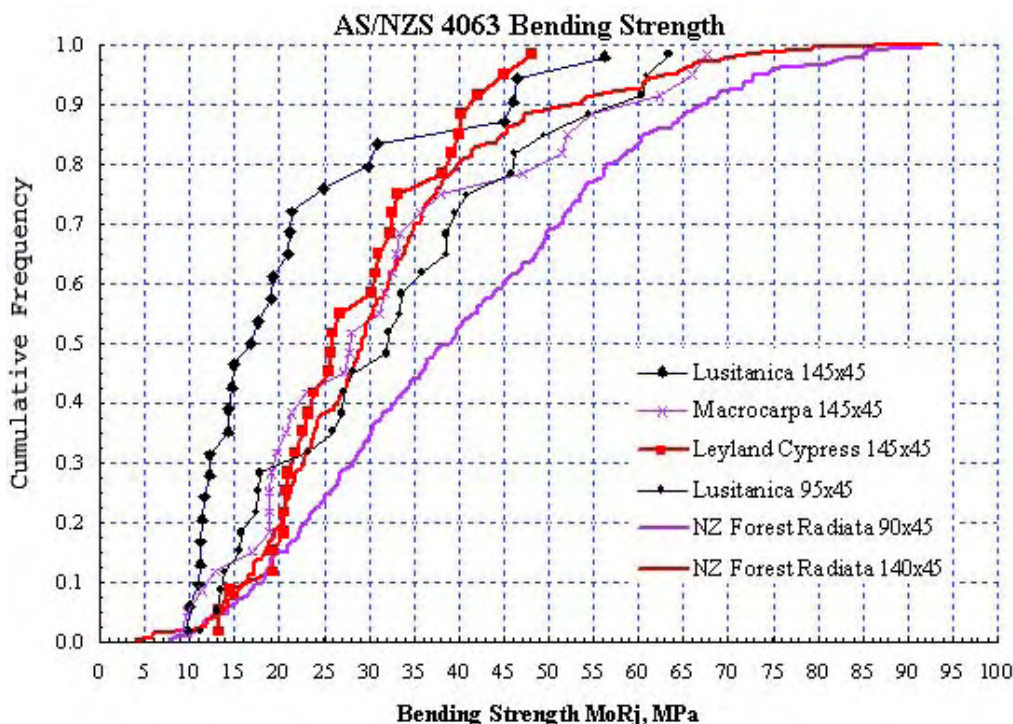
The deficiencies of cypress appearance and structural lumber that have been shown in this study could be alleviated to some extent by a longer rotation, with the addition of more rings of outerwood. In spite of known uniformity of wood density, wood stiffness increases from pith to bark, indicating cypresses do have a juvenile-wood problem. Trees of 300 to 500 mm dbh yielded only 0.2 to 0.6 m³ (representing around 55% recovery) sawn timber at age 21 years. Growing cypresses on such a short rotation negates most of the advantages of cypress timber from older trees over radiata pine, but if a more naturally durable timber is required it could still be done provided appropriate early thinning and pruning were undertaken.

For a full copy of this report see the New Zealand Journal of Forestry Science Vol.35 No.1 (2005).

A pdf is available on www.scionresearch.com under Publications.



Comparison of cumulative frequency distributions of bending strength of radiata pine with cypress species (145 × 45 mm and 95 × 45 mm dimensions)



Comparison of cumulative frequency distributions of bending stiffness of radiata pine with cypress species (145 × 45 mm and 95 × 45 mm dimensions)

ADVANCES IN SCANNING ELECTRON MICROSCOPY FOR IMAGING THE WOOD-COATING INTERFACE

Adya Singh, Anni Ratz, and Bernard Dawson

In a previous Wood Processing Newsletter (Issue No. 36, 2005) we described the novel use of laser confocal microscopy for characterising the plywood-coating interface. As part of on-going tool development for wood finishing research, we present here visual imagery, the fruits of a technique we have developed for examining the wood-coating interface with improved clarity. This technique graphically distinguishes coating from wood tissues. It involves scanning electron microscopy (SEM) backscattered-electron (BSE) images of osmium-tetroxide-stained coated wood sections. The application of osmium tetroxide to the sections results in a reaction only with the coating, dramatically enhancing the contrast and thus the differentiation between coating and wood.

In an Ensis Wood Processing project, the performance of coatings on various wood textures is being investigated. Microscopy is one of several methods we are employing to examine the wood-coating interface in order to assess coating performance, based on fundamental understanding of how coatings interact with wood at the cellular level. Among the microscopy-related developments used, a novel technique involving SEM-BSE imaging of coated-wood sections is the latest technical innovation of value. This technique makes it possible to clearly

differentiate the coating from wood cell walls and thus image the intricate pathways of coating penetration into wood tissues at high resolution. Here we provide illustrations from SEM observations made using the above technique on band-sawn radiata pine plywood that had been coated with an oil-borne penetrating stain.

Sliding microtome cross-sections (90 μm thick) taken through the wood-coating interface were treated with 1% aqueous osmium tetroxide for 4 hours at room temperature. After several washes in water, the sections were briefly rinsed in ethanol and then placed between two glass slides and clamped to air dry. The sections were mounted on stubs with sticky carbon discs, coated with chromium in a vacuum evaporator, and examined with a Jeol field emission SEM (JSM-6400 F) in backscattered electron mode. For comparison, the same sections were also viewed with the SEM operating in the standard imaging (secondary electron) mode.

The secondary electron imaging mode was useful in visualising the extent and nature of surface tissue distortions and cell wall damage that had occurred during band-sawing of the plywood, as illustrated in Fig. 1A and 2A. However, it is apparent from these

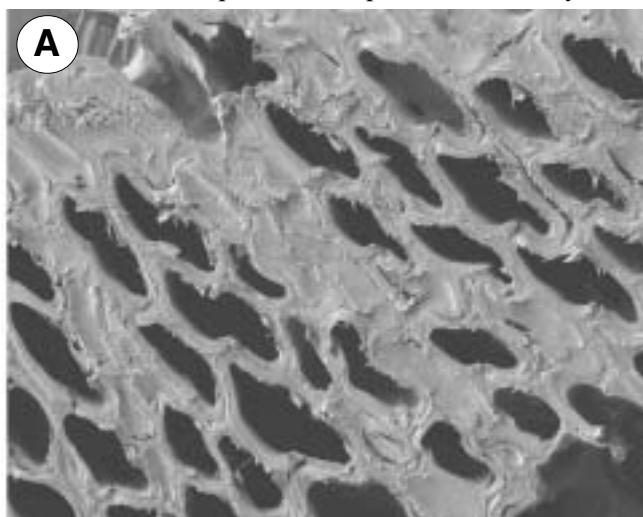
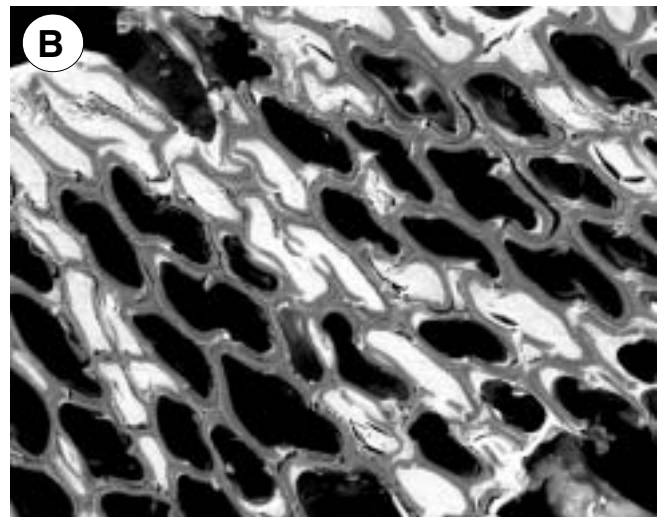


Fig. 1 A: Normal SEM mode.



B: SEM-BSE mode

images that this mode is ineffective for a meaningful observation of the distribution of coating in the surface tissues of the plywood because of a poor contrast between the coating and wood tissues. Backscattered electron imaging proved to be the method of choice, as it was possible to visualise the coating clearly and thus closely follow its distribution within the surface and sub-surface tissues because of excellent contrast differentiation between the coating and wood cell walls (Fig. 1B and 2B).

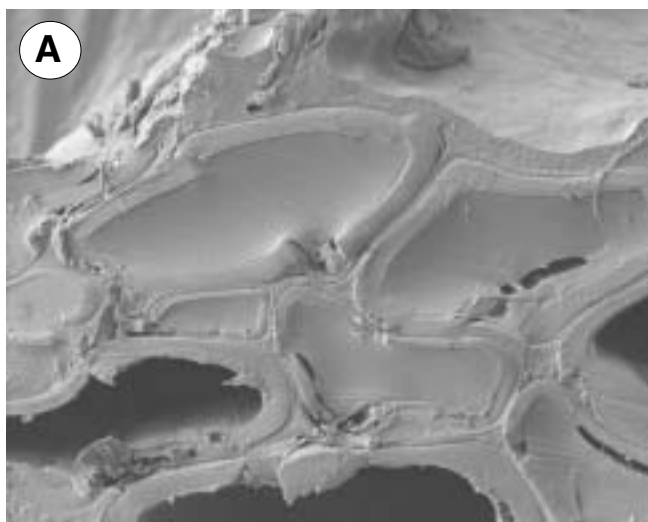
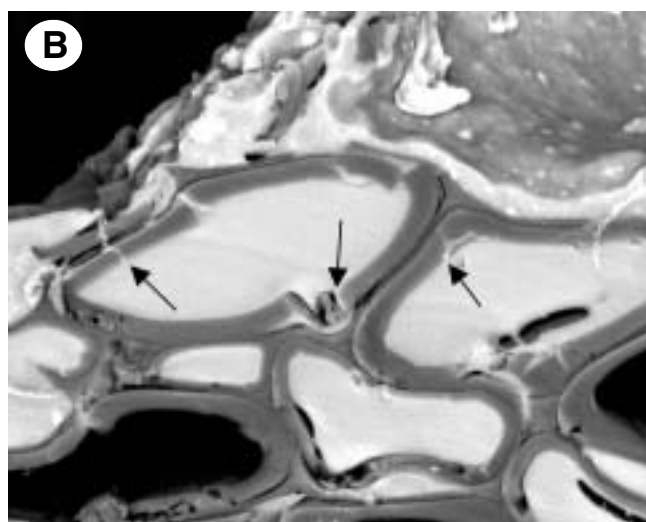


Fig. 2 A: Normal SEM mode

Compared to the non-differentiation normal secondary electron image (Fig 1A), the backscattered electron imaging proved valuable in resolving the intricate pathway of coating penetration into outer tissues, which were damaged from the severe mechanical action of band-sawing (Fig 1B). Virtually every cell seen in Fig. 1B is penetrated by the coating, which is present in the lumina and pit regions, completely filling them in some cells, and in the small voids formed from cracking and delamination of cell walls. At a still greater magnification (Fig. 2A) coating features and wood tissues are seen as indistinguishable, whereas in Fig. 2B, where cells are clearly resolved from the coating, the presence of coating, within even very tiny cracks in cell walls, is recognisable.

In very roughly textured surfaces, such as those seen in the very thin cross-section of Fig. 1 and 2, the distribution of coating within cell lumina and in the cracks in the cell walls can be imagined as a labyrinth of connecting coating which serves to hold surface tissues securely in place over extended periods of exterior weathering. The ability of the roughly textured surfaces to facilitate penetration of lumina, cracks and rupture points, compared with relatively featureless smoothly textured surfaces (e.g., machined



B: SEM-BSE mode

or sanded) demonstrates how rough surfaces are able to accommodate much greater coating loadings than smoother wooden surfaces. And it these much higher coating loadings that are fundamentally responsible for the superior weathering performance of coated roughly textured surfaces compared with smooth surfaces (and more especially so when plywood surfaces are considered).

The illustrations presented here have demonstrated that backscattered electron imaging of osmium tetroxide stained wood sections, for examining the distribution of coating at the wood-coating interface, has proved valuable in significantly advancing our understanding of the wood-coating interface.

A NOVEL APPROACH FOR ENHANCING STIFFNESS OF RADIATA PINE WOOD

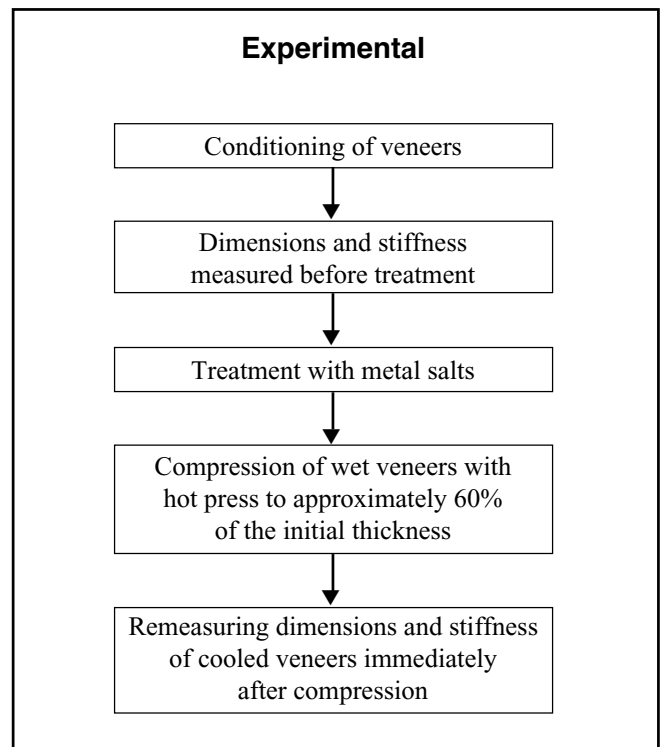
Adya Singh, Tatjana Smolic, and Elizabeth Dunningham

Radiata pine, the most important plantation species in New Zealand, produces average density wood, which lacks the dimensional stability needed in high-performance applications. New Zealand forestry-based industries are keen for us to undertake developments which could lead to substantial improvements in the stiffness and stability of radiata pine wood, enabling it to compete effectively on the international market with species currently considered desirable for high-value applications.

Ensis is making every effort to find solutions to a range of radiata pine wood quality issues which New Zealand forestry industries are facing. One important research area of Ensis-Wood Processing Group is stiffness enhancement of radiata pine wood. The work involves treating the wood with metal salts in combination with heat and compression, and the results obtained to date on the stability and stiffness tests of radiata veneers look promising. Here, we briefly describe the processes used, and some of the test results obtained. Supporting scanning electron micrographs (SEM) taken of uncompressed and compressed radiata pine veneers are included to illustrate the cellular level changes occurring during compression. This information is helpful in understanding the basis for achieving compression fixation and stiffness enhancement.

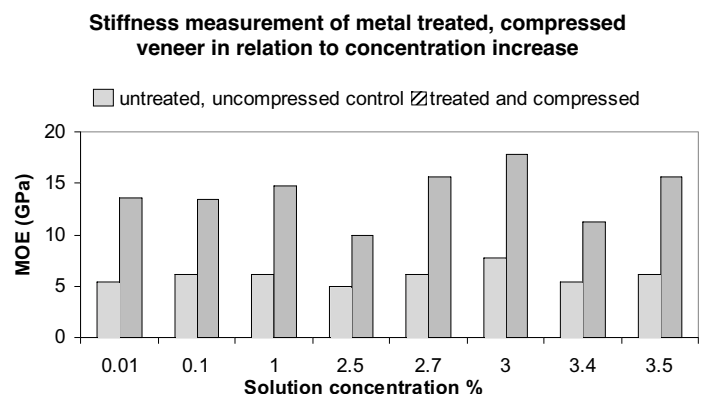
In the preliminary work described in this note we used radiata pine veneers instead of solid wood. Once the methodology has been rigorously tested for its reproducibility in the quality of product achieved, we plan to work with solid wood, including juvenile wood wherever possible. The experimental procedure is summarised in the chart, which describes the steps involved in producing a densified veneer through salt treatments in combination with heat and compression that substantially improved the stiffness, albeit with reduced wood volume. A range of treatment conditions were tried, including different salt concentrations and temperatures during processing. Also, the finished product was rigorously tested for retention of compression by soaking compressed veneers in water for varying periods. In addition, stiffness was measured to compare the effect of various treatments on the stiffness achieved and to identify the conditions that worked best.

The novel approach undertaken in our work, using compression in combination with heat and salt

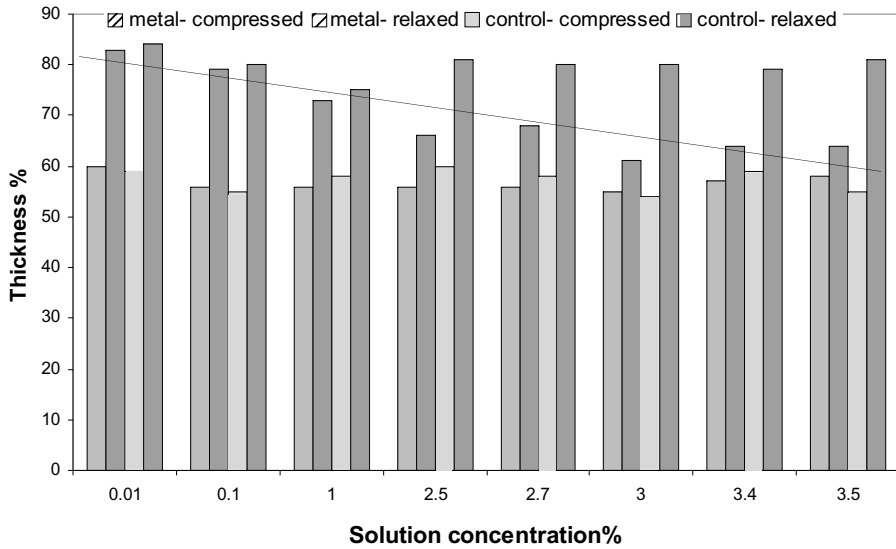


treatment, substantially enhanced the stiffness of radiata pine wood, the main contributing factor being excellent retention of compression. The graphs included show stiffness (MOE) increases in relation to salt concentration and dimensional stability after rigorous water-soak treatment. MOE increased with increasing salt concentrations, with marked gains achieved at all salt concentrations. However, the retention of compression (tested with water-soak treatment) was best achieved at higher salt concentrations, particularly at 2.7% and 3%.

Scanning electron microscopy (SEM) was undertaken to obtain information on the quality of compression achieved, i.e., whether compression occurred throughout the thickness of veneers, and also whether compression occurred uniformly. In addition, SEM



Dimensional stability of treated and control samples before and after water soak



reveals several features related to cell collapse. The initial radial arrangement of axial tracheids is disturbed because of the highly irregular and complex nature of cell wall deformations and attendant cell collapse, resulting in a significant reduction in the volume of cell lumina and consequent increase in the density of wood. Although cell walls are highly deformed, they are largely intact with only minor cracks present in places, an indication that strength losses of compressed veneers are likely to be minimal. Investigations into whether there is any effect on strength are still to be completed and will be reported later.

revealed deformation characteristics of cell walls at both individual cell and tissue levels. This knowledge is of interest from the perspective of understanding the biomechanical behaviour of wood cells during compression. The geometry of wood cells is complex, and it is a challenging task to understand how each cell behaves independently and within a tissue under load.

The SEM micrographs provide a comparison of uncompressed (Fig. 1) and compressed (Fig. 2) veneers, which is helpful in understanding the pattern of compression across the thickness of veneers. The normal appearance of axial tracheids, their radial arrangement, and the morphology and distribution of rays are shown in Fig. 1. In comparison, Fig. 2 provides evidence of compression across the entire thickness of a veneer, although the compression is not uniform, with pockets of tissues showing varying degrees of compression, judging by the extent of cell collapse. The higher magnification view in Fig. 3

It is clear that the technical approaches used for enhancing the stiffness of radiata pine veneers hold promise for future developments. Further progress will come with the use of solid wood, and particularly juvenile wood, which has recognised stability problems.

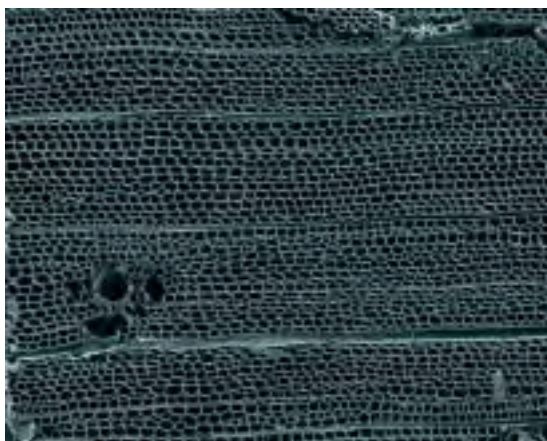


Figure 1. SEM micrograph of uncompressed veneer showing normal appearance of axial tracheids and rays, and radial files of axial tracheids.

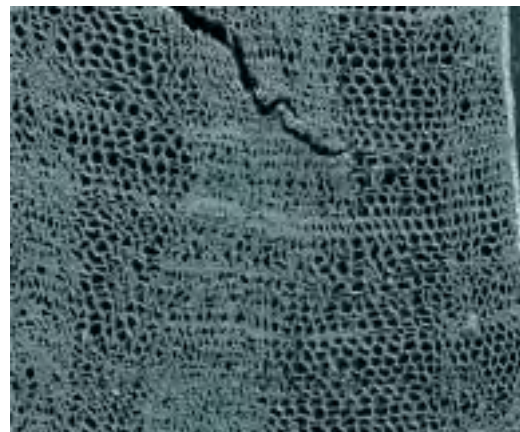


Figure 2. SEM micrograph of metal salt treated compressed veneer showing excellent retention of compression. Note that compression extends across the entire thickness of veneer.

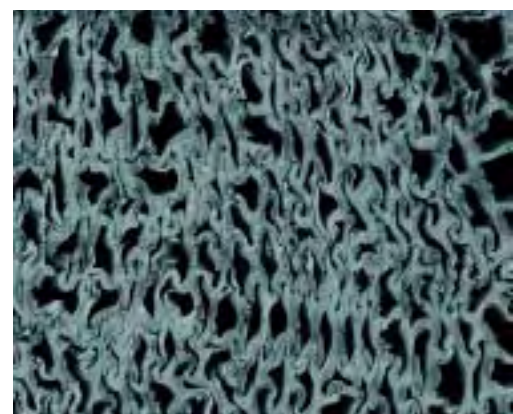


Figure 3. High magnification SEM micrograph of a compressed region. Flattening of cells is evident in some parts. Cell walls are highly deformed but are largely intact with only minor cracks.



Each issue we will delve into our files and give answers to frequently asked drying questions, trying to add to our general understanding of the technical issues behind the art of Wood Drying

BAFFLED ABOUT BAFFLING! WHY IS IT SO IMPORTANT TO BAFFLE MY DRYING STACK?

The short answer is “If you don’t baffle, it will cost”. Without baffles, or with poor baffling, you will either seriously extend your drying time, or increase the cost of achieving the scheduled drying time (by having to put in bigger fans than optimal).

To show why this is so, we need to define “bypass” and demonstrate its effect on performance.

Bypass = Volume of air (m³/s) not passing through the stack, divided by the volume of air (m³/s) passing through the stack.

Air bypassing the stack is air flowing around the packet ends, between car bunks, and under/over stacks. If bearers are used to separate packets vertically, this glut space is classed as bypass if the bearers used are >70 mm deep. This statement about gluts is an Ensis in-house rule of thumb, open to debate.

We have actually tried to measure bypass, by measuring air velocity and flow dimensions in stacks and bypass areas. Results from five kilns are shown in Table 1.

It is apparent that if no attention is paid to baffling, bypass numbers can be high (50–100%). From our experience, bypass less than 30% occurs only where exceptional care is taken, i.e., 20% to 30% is considered normal!

For those who like to delve into the maths, these measured results are confirmed by theory (*see* box).

Calculating bypass:

Empirical bypass results reinforced with a bit of theory. We know that static pressure drop (ΔP) required to achieve a velocity v in a restriction whose aerodynamic resistance is R , is $\Delta P = (\rho R v^2 / 2)$ (where ρ = air density). If we assume that the same pressure drop drives stack and bypass flow, i.e., the bypass and stack act like resistances in parallel, using the fact that volume = $v \times A$, we get

$$\frac{\text{BypassVolume}}{\text{StackVolume}} = \frac{A_B}{A_S} \sqrt{\frac{R_S}{R_B}}$$

From previous work we can estimate flow areas and get R values for stack and bypass areas (use rectangular duct values ¹), and thus get values for our example 2.4-m-wide 60-m³ kiln as in Table 2.

¹ For example “Wood’s Practical Guide to Fan Engineering” 1961

The bypass values in Table 2 cannot be added, as not all bypass zones present themselves to all fans, but they indicate that large bypass values are to be expected and the 50–90 % measured values in Table 1 are in fact highly likely.

Having established likely bypass values, we can now show how they affect performance. In a given kiln, as shown in Newsletter 37 (Dec. 2005) the air delivery in any particular instance is found by the intersection of fan and system pressure/volume (PV) curve. As there

Table 1. Measured bypass from five industrial kilns. In kiln 2, a stack was measured before and after baffling (baffled by nailing plywood and bits of rubber everywhere.)

	1	2a	2b	3	4	5
Stack air velocity m/s	2.7	3.7	5.0	4.7	3.3	2.0
Stack air vol m ³ /s	31.7	36.4	48.7	52.1	33.6	20.1
Bypass air vol m ³ /s	18.1	19.0	0	28.0	16.8	18.5
Bypass ($\frac{\text{BypassVol}}{\text{StackVol}}$)	57	53	0	54	50	92
Comments	Full stack	Full stack	2a fully baffled	Full stack	Full stack	Packet loaded

Table 2. Calculated bypass for our example kiln 2.4 m wide × 60 m³, assuming the equation given in box on page 1.

Flow region	Details of space	Area m ²	R	Bypass %
Stack	2.4×14×3 m (w×l×h) 50 mm boards, 20 mm fillets, 0.6 m spacing	10.82	3.37	
End	0.3 m wide × 3.5 m high	1.05	0.07	67
Under stack	150 mm high, with hobs and bearers	2.1	1.9	26
Top of Stack	300 mm gap	4.2	0.24	145
Between weights	1.2 m gap, 0.25 m thick weights	0.3	0.35	18
Glut spaces	100 × 50 mm glut bearers on edge	3.8	1.83	56

are many kiln types and fan types, it is too difficult to show for a general rule, but we can demonstrate two cases:-

Case 1

In a given kiln designed to have 5 m/s air velocity with 0% bypass, how much extra motor power will I need to achieve 5/m/s at different levels of bypass?

In our example kiln above fitted with 10 × 1.22 m fans, the pressure-volume operating point is 261 Pa at 9.56 m³/sec at 0% bypass. If reversible fans are fitted we would expect 34.3 kW to be drawn at 20°C (assume efficiency = 0.6). As bypass % increases, the volume pushed by the fans must rise proportionally. However, the pressure drop across the stack will be the same, while the pressure drop through the rest of kiln rises with bypass squared. Thus, assuming the designer can adjust the pitch/fan speed to maintain the same fan efficiency, the expected fan performance can be seen in Table 3.

Table 3. An example of the effect of bypass on fan power — assuming the designer manipulates pitch and speed to achieve the same stack velocity.

Bypass %	Pressure drop Pa	Vol/fan m ³ /s	kW for 10 fans
0	261	9.2	34.2
10	302	10.1	43.5
20	347	11.0	54.5
50	502	13.7	98.5
100	829	18.3	216.8

Thus, if kilns are designed to allow for the “normal” bypass, it is at the cost of 2–4 times the electrical energy supplied to the fans. Even at 20% bypass, energy is getting close to doubling.

As a rule of thumb, drying time increases proportionally to the inverse of the square root of air velocity. Table 4 shows that in the “normal” bypass range for the example kiln, air velocity decreases by 15–40 %, which results in an increase in drying time

Case 2

In a given kiln designed to have 5 m/s air velocity with 0% bypass, what actual air velocities will I get at different levels of bypass?

Again this not a trivial question and its answer can only be generally demonstrated here with an example. Using the example kiln/stack configuration, with 10 × 1.22 m diameter fans and a HT sized heat exchanger, each fan delivers 9.17 m³/s at 261.9 Pa, with the stack contributing 56 Pa, if bypass is zero. If the stack is less well baffled, it will have lower resistance in parallel with it. This affects the system curve (as described in Newsletter 37) and thus where it intersects the fan curve, thereby affecting the fan operating point. Figure 1 demonstrates what is happening and gives the three equations which all must be simultaneously solved to find the new pressure volume and stack air velocity, for any value of bypass. The answers are shown in Table 4.

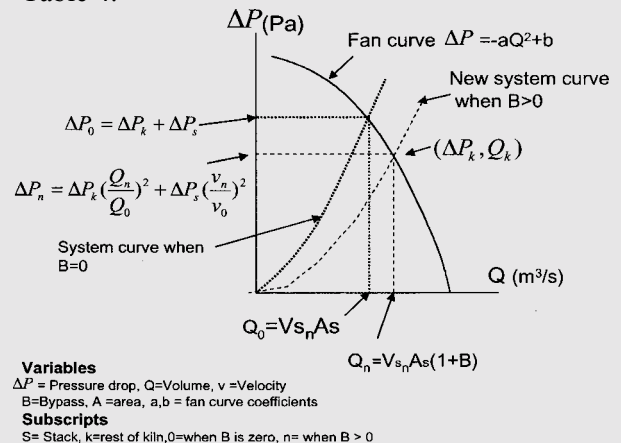


Figure 1. Equations needed to find new operating point and stack velocity as bypass changes

of 8–30%. Note the strong agreement with results for kiln 2 in Table 1.

It is difficult to eliminate bypass totally and practically most people have to live with it being at least 10–20 %. The work presented in this article shows that even at this level, either power costs are ~50% higher or drying times are ~8% longer. It also

Table 4. An example of the effect of bypass level on actual stack air velocity

Bypass %	P Pa	Volum e/fan m ³ /s	Stack air velocity m/s	Drying time increase %
0	261.9	9.17	5.00	0.0
10	257.5	9.27	4.60	4.3
20	254.2	9.35	4.25	8.5
50	247.6	9.50	3.46	20.3
100	242.1	9.63	2.63	38.0

shows that it is very easy to have high bypass levels (50% or more), which can lead to huge cost penalties. For example, a 30 % increase in drying time for a modern HT dryer, using fixed costs alone (at say 18% of capital of \$400k), could be an increase of \$6–8/m³.

Every effort should be made to reduce air bypass in timber kilns. Bypass affects fixed and running costs and any unnecessary bypass is very costly.

WHAT IS THE TEMPERATURE EFFECT ON CAPACITANCE METERS DURING IN-KILN TESTING?

Ian Simpson

It is important to know if capacitance type moisture meters are affected by wood temperature, as they are used to do hot-tests of kiln charges either in the kiln or soon after removal from the kiln. An Ensis study investigated temperature effects using a Wagner L612 capacitance meter. Such meters are almost universally used with their bayonet probe (Wagner L712 stack probe) for in-kiln testing in the Southern Hemisphere softwood industry. Wagner claim that it is “virtually unaffected by temperature” but probably did not envisage its use for in-kiln hot testing.

The study was conducted on boards of 25- and 40-mm-thick, untreated, radiata pine in Ensis research kilns. The boards were dried using three kiln schedules (90/60°, 120/70°, and 140/90°C). For moisture measurement, samples were pulled from the kiln and measured immediately. The relationship



Wagner L612 capacitance moisture meter

between meter reading and oven dry moisture content was determined for each schedule and thickness.

It was found that:

- Readings ARE affected by temperature.
- Timber which is in a hot kiln will give a meter reading which is higher by 1–6% than timber at the same moisture content at ambient temperature.
- The Wagner L612 moisture meter and the Wagner L712 stack probe gave similar readings.
- Timber thickness, kiln schedule, and wood density affected meter readings.
- Error about the prediction line increased with increase in moisture content



Wagner L712 stack probe and capacitance moisture meter

Correction tables are provided here for the two timber thicknesses and the three kiln schedules. The tables include a predicted moisture content for each meter reading, and a 95% LOWER and UPPER confidence interval. These confidence intervals indicate the range the actual moisture content is likely to be within for 95 times in 100 cases.

The Forest Research/Industry 2001-2002 Multiclient Drying Research Group funded this research project.

Table 1. Correction figures for Wagner L612 and Wagner L712 for 40 mm thick timber in a hot kiln on a schedule of 90/60°C.

	If Wagner L612 moisture meter reads:																															
	7	8	9	10	11	12	13	14	15	16	17	18	19	20	21	22	23	24	25	26	27	28	29	30	31	32						
Predicted	3.0	5.1	6.8	8.4	9.8	11.1	12.3	13.4	14.6	15.6	16.6	17.6	18.6	19.5	20.4	21.3	22.1	23.0	23.9	24.7	25.6	26.4	27.2	28.0	28.8	29.5						
Lower	2.8	4.6	6.2	7.8	9.2	10.5	11.7	12.9	14.0	15.1	16.0	17.0	17.8	18.7	19.5	20.2	21.0	21.7	22.3	23.0	23.6	24.2	24.8	25.5	26.2	27.0						
Upper	3.3	5.5	7.4	9.0	10.4	11.7	12.9	14.0	15.1	16.2	17.2	18.2	19.2	20.3	21.2	22.3	23.3	24.3	25.4	26.5	27.6	28.7	29.7	30.6	31.4	32.0						

4

Table 2. Correction figures for Wagner L612 and Wagner L712 for 40 mm thick timber in a hot kiln on a schedule of 120/70°C.

	If Wagner L612 moisture meter reads:																															
	7	8	9	10	11	12	13	14	15	16	17	18	19	20	21	22	23	24	25	26	27	28	29	30	31	32						
Predicted	2.2	4.9	6.7	8.2	9.4	10.6	11.7	12.7	13.7	14.7	15.6	16.5	17.4	18.3	19.2	20.1	21.0	21.8	22.7	23.5	24.3	25.1	25.8	26.5	27.2	27.9						
Lower	0.8	4.1	6.2	7.7	9.0	10.2	11.2	12.2	13.1	14.0	14.9	15.7	16.6	17.4	18.2	19.0	19.6	20.3	20.9	21.5	22.2	22.8	23.4	24.1	24.7	25.3						
Upper	3.6	5.7	7.2	8.6	9.8	11.0	12.2	13.2	14.3	15.3	16.2	17.2	18.2	19.1	20.1	21.2	22.3	23.4	24.5	25.5	26.5	27.4	28.2	29.0	29.8	30.5						

Table 3. Correction figures for Wagner L612 and Wagner L712 for 40 mm thick timber in a hot kiln on a schedule of 140/90°C.

	If Wagner L612 moisture meter reads:																															
	7	8	9	10	11	12	13	14	15	16	17	18	19	20	21	22	23	24	25	26	27	28	29	30	31	32						
Predicted	2.6	5.0	6.6	8.0	9.2	10.4	11.5	12.7	13.8	15.1	16.4	17.9	19.6	21.4	23.0	24.5	25.8	26.8	27.7	28.4	29.0	29.5	-	-	-	-						
Lower	1.3	4.3	6.1	7.5	8.6	9.5	10.4	11.0	11.6	12.2	12.7	13.3	14.2	15.4	17.1	18.8	20.4	21.9	23.2	24.3	25.2	26.1	-	-	-	-						
Upper	3.8	5.6	7.1	8.4	9.8	11.2	12.6	14.3	16.0	18.0	20.1	22.5	25.0	27.3	29.0	30.2	31.2	31.8	32.3	32.6	32.8	33.0	-	-	-	-						

BIOACTIVE RESEARCH AT ENSIS

Tripti Singh, Colleen Chittenden, and Adya Singh

Ensis has initiated a substantial programme intended to develop eco-friendly wood protection systems, and we are currently screening a range of bioactive molecules for their antifungal activity.

Our preliminary studies with chitosan (1-4 linked heterogeneous polymers of glucosamine and N-acetyl glucosamine), which is derived mainly from deacetylation of chitin, have shown that this natural product is highly active against fungi that cause sapstaining of radiata pine logs. Chitin is abundantly present in nature, crustacean shells being a major source, and thus chitosan can be made available for use at relatively low costs. In parallel with continuing screening of other bioactive molecules, our focus is on understanding how the chitosan molecule works at the cellular level because there is little information available on the mode of action of chitosan, although it has been known for a long time that this molecule is active against fungi as well as bacteria. Fundamental knowledge about chitosan action will be important for us in optimising conditions for use of chitosan for effectively controlling sapstaining fungi, as well as in exploring its other uses in industries that are important for the New Zealand economy. The significance of the direction of our work in bioactive research is highlighted by the results obtained to date.

The bioactivity of chitosan was tested against a range of sapstain, mould, and decay fungi using nutrient medium amended with different concentrations of chitosan. Results showed that chitosan is active against wood-degrading fungi but the degree of activity varied with different groups of fungi, decay fungi being most tolerant. The activity was also dependent on the concentration, formulation, and molecular weight ranges. Solubilised, low-molecular-weight chitosan was most effective in inhibiting the growth of test fungi. Based on the initial results, chitosan oligomers (CODP 14) were prepared, which showed enhanced bioactivity when tested for spore germination percentage against two sapstain fungi (*Sphaeropsis sapinea* and *Leptographium procerum*) and a mould fungus, *Trichoderma harzianum* (Fig 1).

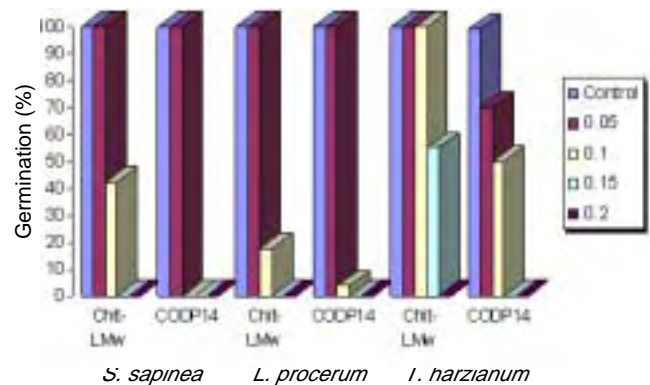


Fig. 1. Fungal germination of three fungi, in medium amended with different concentrations (range 0.05–0.2%) of low molecular weight chitosan and chitosan oligomer (CODP 14).

The effect of chitosan on the morphology and ultra-structure of *S. sapinea* and *T. harzianum* was examined using a range of microscopic techniques. Light microscopy revealed excessive branching in chitosan-exposed mycelium compared to the control. Transmission electron microscopy (TEM) revealed that fungal cells were damaged at all concentrations of chitosan used, and even the lowest concentration of 0.01% effectively destroyed cell structures, including the plasma membrane (Fig. 2), judging by comparison

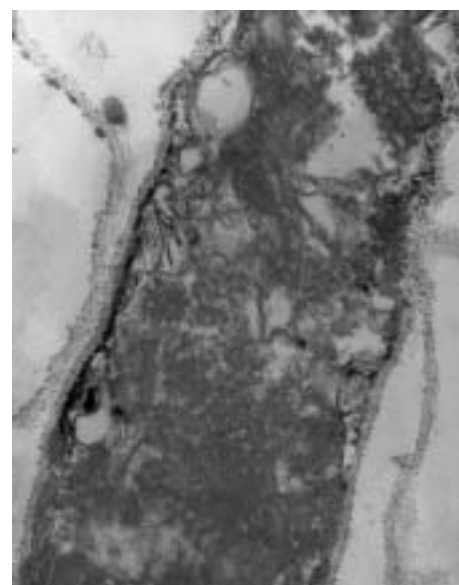


Fig. 2. TEM of hyphae of *S. sapinea* treated with 0.01% chitosan.

with the cell organisation of the untreated (control) fungus, which had intact plasma membrane and normal appearing other structures (Fig. 3). The extent of K^+ leakage from the treated cells provided confirmation that the integrity of the plasma membrane was affected by chitosan.

The fundamental aspect of our future work will involve a time-course study using the lowest effective concentration of chitosan so that we can monitor changes in the ultrastructural organisation of cells and identify chitosan's primary cellular target(s).

Another important component of our work is to develop an integrated protection system, combining natural products such as chitosan with biocontrol agents, which could be applied in-forest for the timely control of detrimental fungi. An application by Ensis for the patent of this work is presently under review.



Fig. 3. TEM of hyphae of untreated *S. sapinea*.

HEAT STERILISATION OF TIMBER FOR EXPORT

Ian Simpson and Steve Riley

Recently Ensis has received enquiries related to heat treatment for timber to meet the quarantine requirements of the importing country. It was felt timely to review heat sterilisation options.

Sterilisation of timber for export is important to many companies in New Zealand and Australia. Many overseas markets impose restrictions on the import of timber products, due to the risk of import of hazards such as insects and fungi. Options for sterilising timber for export include fumigation, preservative treatment, kiln drying, and heat sterilisation. This article focuses on kiln drying and heat sterilisation of sawn timber.

Sterilisation requirements for timber vary from country to country, and specific requirements can be obtained from Biosecurity New Zealand at www.biosecurity.govt.nz. Requirements should be confirmed regularly as they can change without notice. It was the recent (February 2006) inclusion of heat treatment requirements for exporting green sawn Douglas fir timber to Australia that prompted the initial enquiries to Ensis on how to achieve the sterilisation requirements.

Frequently export markets for timber specify a temperature and exposure time, although some may not be specific. There may also be restrictions on the

moisture content of the timber. Sterilisation temperatures may be achieved during kiln drying, but timber that is air dried, or dried in dehumidifiers or low-temperature kilns, may need an additional heat sterilisation step.

There are three main categories relating to timber sterilisation:

- Sawn/machined green timber.
- Sawn/machined dry timber (usually <20% moisture content).
- Packaging timber (green or dry).

These may require different heat treatment to meet the import quarantine regulations of specific countries.

Wooden packaging material in many export markets must meet International Phytosanitary Standards ISPM 15. This standard requires a minimum wood core temperature of 56°C for at least 30 minutes.

For Australia, imported timber must comply with one of two requirements:

- (1) Kiln Drying for quarantine purposes (T9912) requires that the timber should be heated at a dry bulb temperature (DB) of a minimum of 74°C and a WB depression less than 2°C, such that the core temperature achieves a minimum of 74°C. The treatment time varies with thickness from

4 hours for 25 mm, to 18 hours for 200 mm thick timber (larger sizes will require even longer heating times).

OR

(2) Heat treatment (T9968) – for Green sawn timber and packaging materials:

- 56°C for 30 minutes, measured at the core of the wood.
- For acceptance this must be provided by an accredited operator.

For the USA, imported sawn dried radiata pine and Douglas fir must be dried such that the temperature of the centre of each piece of timber is raised to at least 71.1°C, for at least 75 minutes, and the moisture content must be ≤ 20%.

Green sawn timber that is not covered by written confirmation that it will be kiln dried within 30 days of arrival in the USA is not allowed entry under their current regulations.

KILN DRIED TIMBER

Previous Ensis research into kiln drying of radiata pine and Douglas fir has shown the following:

Kiln drying at temperatures above 90°C

Core temperature of 42-mm-thick radiata pine reaches over 70°C within 2 hours when drying at 90/60°C (ACT) (Figure 1). Since drying then continues for approximately 30 hours, it is generally accepted all heat sterilisation criteria would be met (thicker sizes would take longer to reach core temperature limits, but then are dried for a correspondingly longer time). Added to this is the fact that post-drying steaming (conditioning) is usually undertaken, and that during steaming at temperatures >90°C, high core temperatures are attained (Figure 2, Multiclient Drying Research Group 1988). Since HT drying has even higher WB temperatures than ACT drying, it is certain that HT drying also meets all requirements for wood core temperatures.

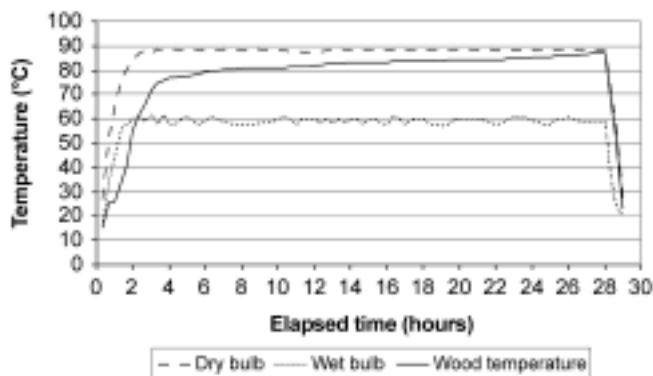


Figure 1. Wood core temperature during drying at 90/60°C.

Achieving core temperatures:

The temperature reached by the core of a piece of wood being dried or heat treated depends on:

- The air DB and WB temperatures (wood tends to rapidly reach the WB temperature and then drift toward the DB temperature).
- Air velocity (a lesser effect).
- The time at those temperature/velocity conditions.
- The wood dimensions.
- The moisture content of the wood at the start of the treatment.

Conventional Temperature (CT, <80°C) and Low Temperature (LT, <60°C) drying.

If a WB depression of less than 2°C with DB greater than 74°C (or 71°C for USA) can be achieved in the kiln for the required time, then go for it. However, if not, then a heat treatment is required by some other means. For CT kilns with steam sprays or water baths, this is straightforward. For LT and dehumidifier dryers there are a host of issues and sensibly it is probably best to find an operator with facilities who can achieve the required conditions.

AIR-DRIED/GREEN TIMBER

To meet any of the export requirements, a heat treatment is required for air-dried or green timber. Existing kilns could be used, with an appropriate heat treatment schedule. Some kiln chambers have wood sensors to measure core temperature (usually to meet ISPM 15 requirements).

Two previous research studies gave possible schedules using steam. Results from a study to measure heatup rates for different-sized green timber

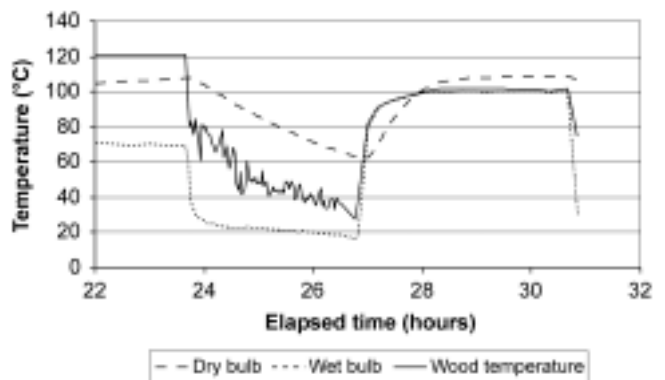


Figure 2. Wood core temperature during cooling and final steaming.

(Research Leaflet No. 34, NZFS 1972) are shown in Figure 3.

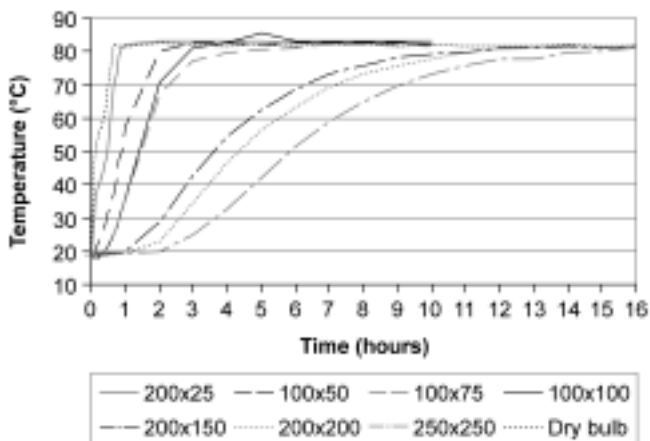


Figure 3. Heat treatment at 82/81, 2.5 m/s, green filleted stack.

More recently a study was conducted for VP NZ Ltd to determine heat sterilisation times for air- and dehumidifier-dried, NZ-grown, 25-mm filleted western red cedar, for export to the US (Figure 4). Steaming was done at 75°C. A 1-hour heat up rate was recommended giving slight surface checking, no collapse, and a small moisture content reduction.

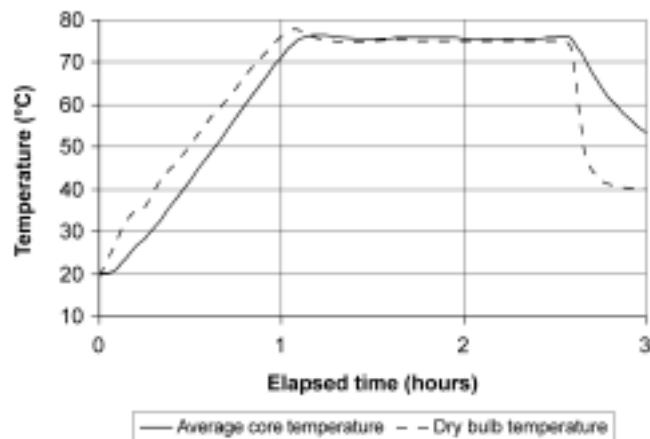


Figure 4. Average wood core temperature of western red cedar boards steamed at 75/75°C.

Points to consider if trying to heat treat in an LT chamber:

- If there is no steam it is difficult to achieve a low WB depression, especially when the wood is dry. Water sprays could be considered but there are some major issues which will be discussed in a future article.
- Is the building insulation able to withstand such conditions?
- Can the sensor measure a WB depression of $<2^{\circ}\text{C}$ (RH is $>92\%$). Most non-WB sensors do not like high humidity, so check with the supplier.
- Often extra heat is made available for heat treatment (e.g., electric resistance heaters in dehumidifiers), but with no humidity it is difficult to determine the time required, and whether damage/over drying of the wood will occur.

WOOD PROCESSING CONTACTS

AREA OF EXPERTISE	NAME
Sawmilling	John Roper (NZ) Russell Washusen (Aus)
Log Quality / Grade Recovery	John Roper (NZ) Russell Washusen (Aus)
Timber Grading / Timber Utilisation	John Turner / Doug Gaunt (NZ) Russell Washusen (Aus)
Remanufacturing	Jeremy Warnes / John Turner (NZ)
Wood Quality	Dave Cown (NZ)
Alternative Species (to radiata)	John Roper / Russell McKinley (NZ) Russell Washusen (Aus)
Timber Drying	Steve Riley (NZ) Richard Northway (Aus)
Timber Engineering	Doug Gaunt (NZ) Richard Northway (Aus)
Kiln Design / Kiln Control / Dryspec	Steve Riley / Richard Dandoroff (NZ) Richard Northway (Aus)
Preservation and Antisapstain Treatments	Mick Hedley (NZ) Laurie Cookson (Aus)
Bioenergy	Per Nielsen (NZ)

CONTACTING Ensis

Ensis Australia

Telephone: +61 3 9545 8100

Freephone (within Australia only): 1800 231 051

Facsimile: +61 3 9545 2223

Bayview Avenue
Clayton, Vic 3168
Private Bag 10
Clayton South, Vic 3169
Australia

www.ensisjv.com
enquiries@ensisjv.com

Ensis New Zealand

Telephone: +64 7 343 5777

Freephone (within NZ only): 0800 231 051

Facsimile: +64 7 348 0952

Te Papa Tipu Innovation Park
49 Sala Street
Private Bag 3020
Rotorua 3046
New Zealand

Ensis is an unincorporated joint venture between CSIRO FFP Pty Ltd and Scion Australasia Ltd. Disclaimer: Ensis shall not be liable for technical or editorial omissions contained herein. The information is provided in the best of faith but is subject to change without notice.



THE JOINT FORCES OF CSIRO & SCION